MEDWIN PUBLISHERS
Committed to create value for Researchers

Petroleum & Petrochemical Engineering Journal
ISSN: 2578-4846

Exploitation of Heterostructure Photocatalyst Impregnated Alginate Beads for Enhanced Removal of Methyl Orange under Solar Light

Motawea EA* and Ali HR

Spectroscopic Division, Analysis and Evaluation Department, Egyptian Petroleum Research Institute, Cairo, Egypt

***Corresponding author:** Eman A Motawea, Spectroscopic Division, Analysis and Evaluation Department, Egyptian Petroleum Research Institute, Cairo, Egypt, Tel: 01227024388; Email: eman.chemie@gmail.com

Research Article

Volume 2 Issue 8

Received Date: November 21, 2018

Published Date: December 10, 2018

DOI: 10.23880/ppej-16000180

Abstract

In the current study, composite photocatalyst of Ag_3Po_4-Ag_2CO_3 impregnated in alginate beads was synthesized by co-precipitation method and characterized by XRD, FTIR and SEM analyses. Photocatalytic activity of the synthesized impregnated beads was evaluated by degradation of methyl orange (MO) under sun light. The suggested parameters as PH(3-9) and catalyst dosage (0.5-3.5 g/l) were studied using the Response Surface Methodology (RSM) and the optimum conditions were as follows: pH=3and catalyst dosage= 2 g/l. And the methyl orange (MO) removal efficiency reached up to 67.9 % at these optimal conditions. Also kinetic and isotherm of the Photocatalytic degradation were determined in order to more completely understand the degradation mechanism.

Keywords: Photocatalytic efficiency; Ag_3Po_4-Ag_2CO_3; Sodium alginate beads; Heterogenous catalyst

Introduction

Until the end of the nineteenth century, pigments were used to be extracted from natural substances, such as flowers, roots, and minerals. With the development of modern synthetic chemistry and chemical industry, natural dyes have been replaced by synthetic ones because they can be manufactured on a larger scale, however, this process represents a great threat for our environment and human health [1-4]. Therefore, the removal of polluting dyes from the wastes of industries before they get in contact with the environment is a mandatory step to reduce the pollution [5]. Methyl orange (MO) is commonly used mono azo dyes in laboratory assays, textiles and other commercial products, and have to be removed from water due to its toxicity [6-8]. Considering factors such as cost and efficiency, a great deal of visible-light-responsive photocatalysts including many binary/ternary semiconductors, such as WO_3, CdS, MoS_2, g-C_3N_4, Ag_3PO_4 and $BiVO_4$ have been developed over the past decades [9-13]. Environmental problem of toxic wastewater and infected waters is one of the main subjects that researchers work on. Due to this, organic dyes are one of the main industrial wastewater pollutions. More than 50% of textile dyes is azoic dyes such as methyl orange which are recognized by nitrogen π-bound

[1-2]. Of the total world production of dyes, up to 20% is lost during industrial processing, causing environmental pollution and contributing to eutrophication that affects aquatic life [14]. This necessitates to degrading the dyes in effluents, at least to decolorize them before effluent disposal to environment. So far, many strategies have been designed to clear the dyeing effluents. Photocatalytic degradation of organic pollutants by using semiconductor photocatalysts is of growing interest for water purification [15-16]. It is a potential technology for the destruction of organic contaminants in water such as aromatic compounds which present a potential hazard to the environment. Methyl orange (MO) was used as a model compound, we performed our strategy by taking MO degradation as an example. Photocatalysis is a technique utilizing nanotechnology under thorough study now [5-7]. The process of photocatalysis is powered by photons that match or exceed the band gap energy of a given semiconductor. An electron in its valence band (VB) is excited to the conduction band (CB), leaving a positive hole in the VB that forms a hydroxyl radical with the hydroxyl ion in water, which is then available for oxidation. Meanwhile, the excited electron reduces oxygen in the CB, which can also act as an oxidizing agent [8]. However, the photogenerated electrons are unstable in the excited state, thus can easily recombine to their respective holes. This process dissipates the input light energy and results in low-efficiency photocatalysis. Therefore, the development of a more efficient photocatalyst is an important consideration [8-10]. Oxidation of organic compounds in aqueous solution is achieved by the reactive hydroxyl radical. The primary oxidant responsible for most heterogeneous photocatalytic oxidation (HPCO) processes is the hydroxyl radical, which is formed by the reduction reactions of holes with water or hydroxide ions. The mechanism of the formation of the hydroxyl radical is well discussed in the literature [17-22]. Ag_2CO_3 has been confirmed to exhibit a high photocatalytic activity for organic pollutant degradation, because the incorporation of a nonmetallic p-block carbon element into Ag_2O can broaden the band gap, which can enhance the redox ability [23]. Therefore, Ag_2CO_3, as a p-type semiconductor, can form a p–n heterojunction with Ag_3PO_4, which is an n-type semiconductor. However, the used of Ag_3PO_4 powder is limited to simple applications because significant post treatment filtration is required to remove the catalyst from the final solution. Therefore, many researches undertook many attempts to entrap photocatalyst particles in some supports for degradation of dyes and adsorption of heavy metal ions, such as entrapping TiO_2 in PVA-alginate [10] or chitosan [11-12]. These materials could provide considerable advantages: minimal clogging in continuous flow systems, easier solid-liquid separation and ease of regeneration and reuse of the catalyst. Alginate is naturally occurring linear polysaccharide composed of (1-4)-linked-D-mannuronic acid (M units) and –L-guluronic acid (G-units) monomers, which vary in amount and sequential distribution along the polymer chain depending on gelling properties [24-28]. In the present study, Ag_3PO_4/ Ag_2CO_3 impregnated alginate beads were prepared. The removal of dyes using the aforementioned beads has not been extensively explored. Thus, the aim of this study was to improve the performance of dye removal by using photocatalyst beads containing Ag_3PO_4/ Ag_2CO_3. The optimum conditions, kinetic and isotherm of dye removal were determined. Until the end of the nineteenth century, pigments were used to be extracted from natural substances, such as flowers, roots, and minerals. With the development of modern synthetic chemistry and chemical industry, natural dyes have been replaced by synthetic ones because they can be manufactured on a larger scale, however, this process represents a great threat for our environment and human health [1-4]. Therefore, the removal of polluting dyes from the wastes of industries before they get in contact with the environment is a mandatory step to reduce the pollution [5]. Methyl orange (MO) is commonly used mono azo dyes in laboratory assays, textiles and other commercial products, and have to be removed from water due to its toxicity [6-8]. Considering factors such as cost and efficiency, a great deal of visible-light-responsive photocatalysts including many binary/ternary semiconductors, such as WO_3, CdS, MoS_2, g-C_3N_4, Ag_3PO_4 and BiVO4 have been developed over the past decades [9-13]. Environmental problem of toxic wastewater and infected waters is one of the main subjects that researchers work on. Due to this, organic dyes are one of the main industrial wastewater pollutions. More than 50% of textile dyes is azoic dyes such as methyl orange which are recognized by nitrogen π-bound [1-2]. Of the total world production of dyes, up to 20% is lost during industrial processing, causing environmental pollution and contributing to eutrophication that affects aquatic life [14]. This necessitates to degrading the dyes in effluents, at least to decolorize them before effluent disposal to environment. So far, many strategies have been designed to clear the dyeing effluents. Photocatalytic degradation of organic pollutants by using semiconductor photocatalysts is of growing interest for water purification [15,16]. It is a potential technology for the destruction of organic contaminants in water such as

aromatic compounds which present a potential hazard to the environment. Methyl orange (MO) was used as a model compound, we performed our strategy by taking MO degradation as an example. Photocatalysis is a technique utilizing nanotechnology under thorough study now [5-7]. The process of photocatalysis is powered by photons that match or exceed the band gap energy of a given semiconductor. An electron in its valence band (VB) is excited to the conduction band (CB), leaving a positive hole in the VB that forms a hydroxyl radical with the hydroxyl ion in water, which is then available for oxidation. Meanwhile, the excited electron reduces oxygen in the CB, which can also act as an oxidizing agent [8]. However, the photogenerated electrons are unstable in the excited state, thus can easily recombine to their respective holes. This process dissipates the input light energy and results in low-efficiency photocatalysis. Therefore, the development of a more efficient photocatalyst is an important consideration [8-10]. Oxidation of organic compounds in aqueous solution is achieved by the reactive hydroxyl radical. The primary oxidant responsible for most heterogeneous photocatalytic oxidation (HPCO) processes is the hydroxyl radical, which is formed by the reduction reactions of holes with water or hydroxide ions. The mechanism of the formation of the hydroxyl radical is well discussed in the literature [17-22]. Ag_2CO_3 has been confirmed to exhibit a high photocatalytic activity for organic pollutant degradation, because the incorporation of a nonmetallic p-block carbon element into Ag_2O can broaden the band gap, which can enhance the redox ability [23]. Therefore, Ag_2CO_3, as a p-type semiconductor, can form a p–n heterojunction with Ag_3PO_4, which is an n-type semiconductor. However, the used of Ag_3PO_4 powder is limited to simple applications because significant post treatment filtration is required to remove the catalyst from the final solution. Therefore, many researches undertook many attempts to entrap photocatalyst particles in some supports for degradation of dyes and adsorption of heavy metal ions, such as entrapping TiO_2 in PVA-alginate [10] or chitosan [11-12]. These materials could provide considerable advantages: minimal clogging in continuous flow systems, easier solid-liquid separation and ease of regeneration and reuse of the catalyst. Alginate is naturally occurring linear polysaccharide composed of (1-4)-linked-D-mannuronic acid (M units) and –L-guluronic acid (G-units) monomers, which vary in amount and sequential distribution along the polymer chain depending on gelling properties [24-28]. In the present study, Ag_3PO_4/ Ag_2CO_3 impregnated alginate beads were prepared. The removal of dyes using the aforementioned beads has not been extensively explored. Thus, the aim of this study was to improve the performance of dye removal by using photocatalyst beads containing Ag_3PO_4/ Ag_2CO_3. The optimum conditions, kinetic and isotherm of dye removal were determined.

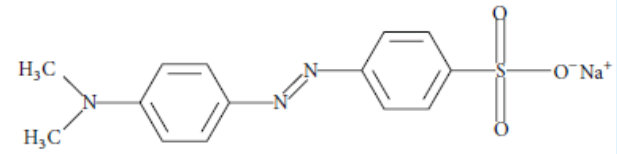

Figure 1: Chemical structure of methyl orange.

Experimental Section

Synthesis of Photocatalyst Heterostructure Ag_3PO_4/Ag_2CO_3

All chemicals were of analytical grade purity and used without further purification. Briefly, 252 mg $NaHCO_3$ and 312 mg $NaH_2PO_4{\cdot}2H_2O$ were dissolved in 80 mL deionized water understirring. Then, 40 mL $AgNO_3$ aqueous solutions (approximately 0.3 mol/L) was added drop wise to the solution under stirring. The precipitate was collected by centrifugation, washed three times with deionized water after stirring for 12 h and dried in air at 70°C for 12 h [29].

Preparation of Photocatalyst Heterostructure Embedded in Polymeric Beads

About 300 mL of precursor solution was prepared by mixing 9 g of sodium alginate powder with deionized water (4.0% w/v solution) at 60°C. After the dissolution, 1.5 g of Ag_3PO_4 /Ag_2CO_3 powder in deionized water (DI) was added very slowly and the mixture was further stirred for 3.0 h to ensure the homogeneity of the system. The obtained viscous solution was introduced dropwise using a syringe into 400 mL of a $CaCl_2$ solution (4% (w/v)) bath as the gelling solution [30]. The beads were cured in the coagulation bath overnight. Then, the beads were washed several times and kept in a deionized water bath. The beads were used wet to avoid the collapse of the internal structure.

Characterization of the Catalyst

XRD measurements were obtained using a Shimadzu XRD-600 diffractometer operating at a voltage of 40 kV

and current of 20 mA with Cu Ka radiation source. The infrared spectra were analyzed using Fourier transform infrared (FTIR) spectroscopy (ATI/Unicam Infinity 961 M instrument) in the range of 4000–400cm^{-1}. The surface morphology and porous structure was examined using scanning electron microscopy (SEM) (JEOL 5410) and the power was set to 30 kV.

Photocatalytic Degradation of Methyl Orange and Design of Experiments (DOE)

The effect of degradation process parameters such as pH(3-9) and catalyst dosage(0.5-3.5) on the removal efficiency of methyl orange (MO) onto Ag_3PO_4 /Ag_2CO_3 alginate beads was optimized by response surface methodology (RSM) based central composite design (CCD). The CCD model was used to investigate the combination of parameters that will give optimum removal.

Factors			Levels		
	-α	-1	0	+1	+α
Catalyst dosage (g/20ml)	0.5	1	2	3	3.5
pH	3	4.5	6	7.5	9

Table1. Experimental factor levels of Ag_3PO_4 /Ag_2CO_3 alginate beads

The batch photocatalytic experiment was performed in methyl orange (MO) under sunlight irradiation. Ag_3PO_4 /Ag_2CO_3 alginate beads (wet weight) were introduced into 20 mL of MO solution (25 ppm). The mixture was stirred in the dark for 120 min to attain adsorption-desorption equilibrium between the catalyst and dye. The mixture was then irradiated under sunlight in sunny condition.

The degree of photodegradation (efficiency) as a function of time, which demonstrates the efficiency of the experiment, could be calculated with the following equation:

$$RE = \left(\frac{C_{o-Ce}}{C_o}\right) \times 100 \ (1)$$

Where C_o and Ce (mg/l) are the initial and final methyl orange (MO) concentrations, respectively.

Kinetic Modeling

The data were treated according to the pseudo-first-order, pseudo-second-order [10,11] in their linear forms that expressed as:

$$\log(q_e - q_t) = \log(q_e) - (\frac{K_1}{2.303})t \ (2)$$

$$\frac{t}{q_t} = \frac{1}{(K_2\ q_e^2)} + \left(\frac{1}{q_e}\right) t \ (3)$$

Where, q_t and q_e are the amounts of methyl orange adsorbed at time t and equilibrium e, respectively; K_1 and K_2 are the pseudo first-order and pseudo second-order rate constants, respectively.

Isotherm Modeling

Two adsorption isotherm models have been used to analyze the adsorption data by the following equations [12,13]:

(i) Langmuir

$$\frac{C_e}{q_e} = \frac{1}{K_L Q_{max}} + \frac{C_e}{Q_{max}} \ (4)$$

Where, K_L (L/mg) and Q_{max} (mg/g) are the Langmuir constants related to the adsorption energy and sorption capacity, respectively. While, q_e (mg/g) is the equilibrium adsorption capacity and C_e (mg/L) is the equilibrium concentration.

(ii) Freundlich.

$$\log q_e = \log K_f + \frac{1}{n} \log C_e \ (5)$$

Where, K_f (L/mg) is the Freundlich constant and n is the heterogeneity factor which represents sorption capacity and sorption intensity, respectively.

Results and Discussion

Characterization of the Catalyst

The crystallographic structures of algenic acid and the as-prepared sample were examined by X-ray powder diffraction (XRD). As shown in Figure 2 X-ray of algenic acid showed an amorphous structure, while X-ray of the Ag_3PO_4-Ag_2CO_3 sample showed peaks at 18.5° (020), 20.6° (110), 32.6° (101), 33.7° (–130), 37.1° (040) and 39.6° (031) which are indexed to that of monoclinic Ag_2CO_3 (JCPDS 01-073-4385)Further, the crystallite size was calculated using Scherrer's formula for the high intensity peak, the estimated grain size was found to be 87 nm with d-spacing 0.227 nm. The peaks at 21.0° (110),29.8° (200), 33.4° (210), 36.7° (211), 47.9° (310), 52.8° (222),55.1° (320) and 57.4° (321) are indexed to that of cubic Ag_3PO_4 (JCPDS 00-006-0505), the estimated grain size was found to be 81.95 nm with d-spacing 0.16 nm.

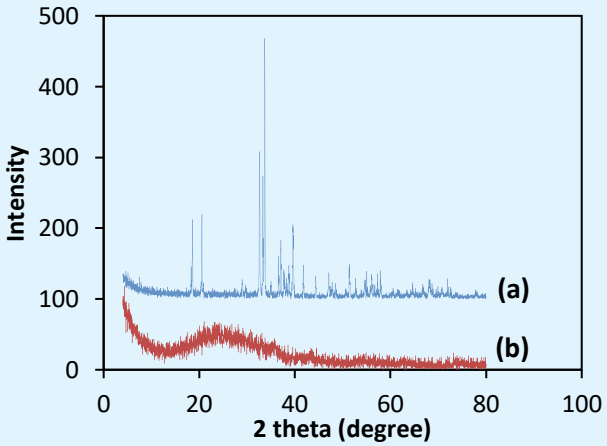

Fig (2): XRD patterns of (a) prepared catalyst and (b) Algenic acid

In FT-IR spectrum of algenic acid Figure 3 a broad peak at 3438–3450 cm^{-1} in the spectrum of alginate and was attributed to the OH groups, the bands at 2918–2923 cm^{-1} in the spectra are attributed to the C-H stretch vibration in alginate [31-33]. Also, the bands at 1630–1648 cm^{-1} and 1410–1440 cm^{-1} observed in the spectra were attributed to the asymmetric and symmetric stretching bands of the O=C–O of alginate, respectively.

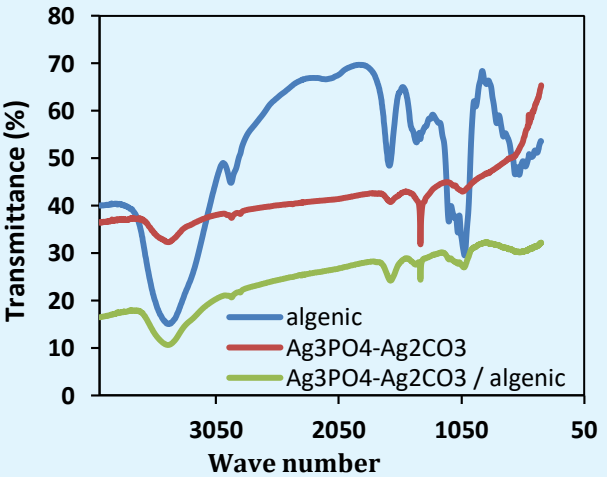

Figure 3: FTIR curves of the prepared materials.

While in the IR spectrum of Ag_3PO_4-Ag_2CO_3 absorption peaks at 567 and 1016 cm^{-1} can be attributed to the stretching vibrations of the PO_4 group [20] which verify the existence of Ag_3PO_4 in the sample, and the peaks around 1600 and3200 cm^{-1} represent the physically adsorbed water on the catalyst surface .the characteristic absorption bands of CO_3^{-2} could be observed at 708 cm^{-1}, 802 cm^{-1}, 883cm^{-1}, 1328 cm^{-1} and 1449 cm^{-1} [34]. Besides, the peaks at 1640cm^{-1} and 1540 cm^{-1} are found and the peak intention of CO_3^{2-}. The IR peaks at 1140 and 1730 cm^{-1} corresponds to C–O and C=O in EGDMA, respectively. In case of Ag_3PO_4-Ag_2CO_3 alginate beads the characteristic C=C peaks at 1630, 1380, and 990 cm^{-1} show low intensity that verified the crosslinking polymerization reaction.

The surface morphology of photocatalyst was examined using scanning electron microscopy. SEM images Figure 4 show particles with a polyhedral morphology similar to rhombic dodecahedral particles of Ag_3PO_4-Ag_2CO_3.

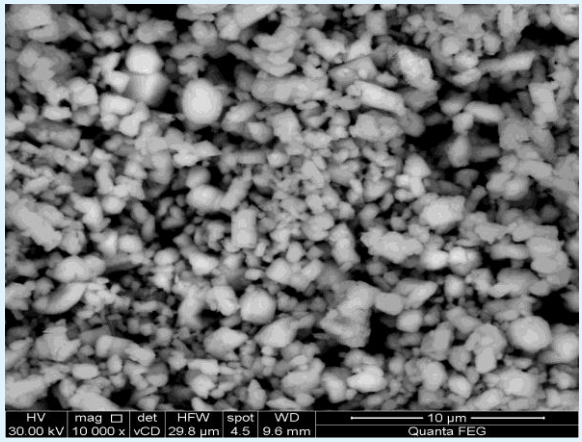

Figure 4: SEM images of Ag_3PO_4-Ag_2CO_3.

Photocatalytic Activity

Design and Optimization: The effect pH (3-9) and catalyst dosage (0.5-3.5) on the removal efficiency of methyl orange (MO) onto Ag_3PO_4 /Ag_2CO_3 alginate beads was investigated using central composite design (CCD), which is a statistical and mathematical technique useful for building models, designing experiments and analyzing the interactive effects of several independent parameters. The main advantage of CCD is to reduce the number of experiments to be conducted, to study the interactions of operations parameters and to optimize the conditions [16].

Adsorbate	Source	DF	SS	MS	F-value	Prob.> F
MO	Model	5	1574.9	314.99	12.08	**0.0399**
	Error	4	1234.2	308.55		
	Lack of Fit	3	1234.2	411.40	863.55	0.5061
	Pure Error	1	0	0		
	Total (Model + Error)	9	2809.1	312.13		

Table 2: ANOVA analysis of response surface for removal of methyl orange (MO) onto Ag_3PO_4 /Ag_2CO_3 alginate beads.

The results for the ANOVA of the response surface quadratic analyses and model terms are summarized in Table 2. The high coefficient of determination value for methyl orange (MO) (R^2 = 0.99) showed that the quadratic modes utilized highly sufficient in predicting the responses.

Also, the F-value of 12.08 of the quadratic model implied that the equation was significant. The values of probability > F was 0.0399 showed model terms were significant. From the model, the predicted methyl orange (MO) removal and optimum conditions by Ag_3PO_4 /Ag_2CO_3 alginate beads (catalyst dosage: 2g/ 20 mL and pH 3.0) with predicted methyl orange (MO) percent removal 68.1%, were obtained. While, the actual methyl orange (MO) percent removal was 67,9%, this indicated the reliability of the models. The increase in the number of active sites on the catalyst surface, causing an increase in the number of absorbed photons, which leads to production of large number of •OH radicals, and increase degradation of Methyl orange molecules similar observation was reported by Saad, et al. [17].

Figure 5 indicated 3D response surface plots of percent removal of methyl orange (MO) as a function of two studied parameters.

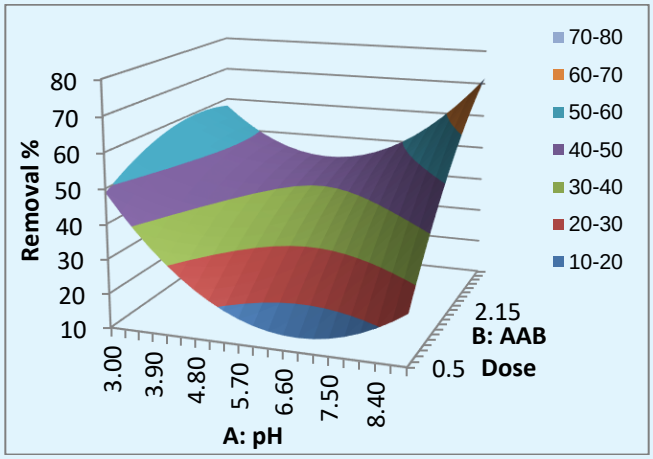

Figure 5: 3D Response surface plot for the combined effect of pH with the effect of catalyst dosage on the removal % of methyl orange (MO) onto Ag_3PO_4 /Ag_2CO_3 alginate beads.

As Wenjun, et al. [35] reported The CB position of Ag_2CO_3 is more negative than that of Ag_3PO_4 and the VB position of Ag_3PO_4 is more positive than that of Ag_2CO_3. Thus, under visible-light irradiation, the excited electrons in the CB of Ag_2CO_3 can rapidly transfer to the CB of Ag_3PO_4. At the same time, photoinduced holes in the VB of Ag_3PO_4 can transfer to the VB of Ag_2CO_3. However, the formation of the p–n heterojunction greatly increases the separation of photoexcited electrons and holes, suppressing electron-hole recombination, which results in the enhanced photocatalytic performance.

Kinetic Modeling

The degradation of organic waste on the alginate supported photocatalyst was initiated by the adsorption of the target molecule on the catalyst surface followed by

photocatalytic degradation [36]. Here, methyl orange (MO) was adsorbed on the Ag_3Po_4-Ag_2CO_3 impregnated in alginate beads surface and simultaneously removed from the system due to the photocatalytic reaction.

The data were treated according to pseudo-first order, pseudo-second order kinetic models, and the obtained results are tabulated in Table 3.

Adsorbate	Kinetic model	Kinetic constants				
		R^2	K_1 (min^{-1})	$q_{e,cal}$ (mg/g)	K_2 (g/mg min)	$q_{e,cal}$ (mg/g)
MO	Pseudo-first order	0.4836	0.010133	1.572		
	Pseudo-second order	0.9998			0.01439539	9.523

Table 3: Kinetic parameters of the pseudo-first and second-order models for the removal of methyl orange (MO) onto Ag_3Po_4-Ag_2CO_3 impregnated in alginate beads (dry weight adsorbent dosage 0.045g/20 mL, initial methyl orange (MO) concentration 25ppm and temperature 25°C).

The kinetic parameters for the pseudo-second order model were determined from the linear plot of t/q_t against t in Figure 6, first-order kinetic model showed low correlation coefficient values R^2 (0.483), this suggested that the pseudo-first-order model was not suitable to describe the process.

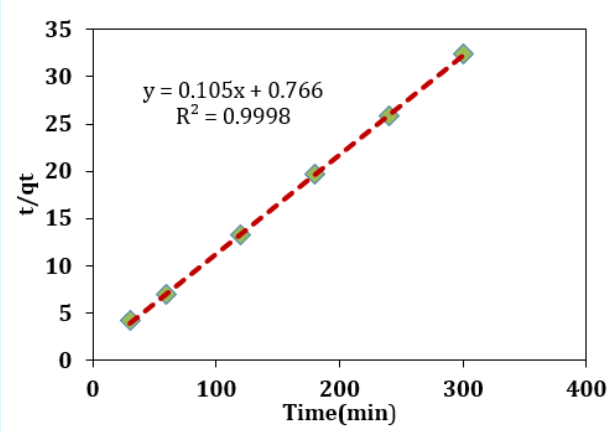

Figure 6: Pseudo-second order kinetic model for the photodegradation of methyl orange (MO) onto Ag_3Po_4-Ag_2CO_3 impregnated in alginate beads (dry weight adsorbent dosage 0.045g/20 mL, initial methyl orange (MO) concentration 25ppm and temperature 25°C).

While, the good linear plots of t/qt vs. t with high correlation coefficients R^2 > 0.99 suggested that the photodegradation of methyl orange (MO) onto catalyst were predominantly followed the pseudo-second-order kinetic model and the chemical reaction occurred between methyl orange and the surface of the catalyst involving valence forces through sharing or exchange of electrons [37,38].

Isotherm Models

The equilibrium data were analyzed using the Langmuir and Freundlich isotherm models Equations 4 and 5. 0.045 gram of the catalyst per 20 mL of methyl orange were used at pH of 3, equilibrium time of 4 h and temperatures of 25 °C to study the photodegradation of 10, 25, 50, 100,150 and 200 mg/L of methyl orange.

The Langmuir model assumes that the photodegradation occurs on a homogeneous surface by monolayer coverage with uniform binding sites, equivalent photodegradation energies. While, the Freundlich isotherm is an empirical equation assuming that the photodegradation process takes place on heterogeneous surfaces and photodegradation capacity is related to the concentration of the catalyst at equilibrium [39,40].

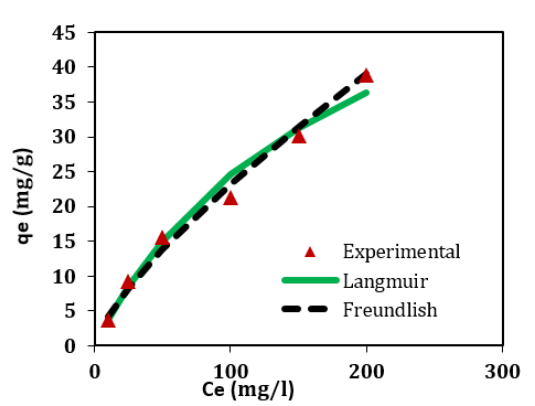

Figure 7: Comparison of the fit of the Langmuir and Freundlich isotherm models for the photodegradation of methyl orange onto Ag_3Po_4-Ag_2CO_3 impregnated in alginate beads (catalyst dosage 0.045g/20 mL, contact time 240 min and temperature 25°C).

A comparison of the fit of the Langmuir and Freundlich equations of methyl orange photodegradation by Ag_3Po_4-Ag_2CO_3 impregnated in alginate beads are shown in Figure 7. Also, their constants along with correlation coefficients (R^2) are depicted in Table 4.

The results revealed that close agreement with the theoretical prediction of Freundlich model, where the photodegradation process takes place on heterogeneous surfaces. Similar observation was reported by Xiong, et al. [41], the high initial dye concentrations could negatively affect the photocatalytic reaction, decreasing the distance photons had to travel before they enter the MO solution. Only a small number of photons could be transferred to the surface of the composite because of the reduction in light penetration at high dye concentrations, that was consistent with previous dye degradation studies using photocatalysts [42-44].

Adsorbent	Isotherm model	Isotherm constants				
		R^2	Qmax	b	Kf	1/n
MO	Langmuir	0.899	68.96	0.00555		
	Freundlich	0.986			1.36	0.75

Table 4: Isotherm parameters of Langmuir and Freundlich models for the photodegradation by Ag_3Po_4-Ag_2CO_3 impregnated in alginate beads (catalyst dosage 0.045g/20 mL, contact time 240 min and temperature 25°C, initial concentration of 10, 25, 50, 100,150 and 200 mg/L methyl orange).

Conclusions

In this research, application of algenic polymer (algenic beads impregnated/Ag_3PO_4-Ag_2CO_3) for enhanced removal of Methyl orange under solar light was investigated. The results indicate that the optimum conditions was (catalyst dosage: 2g/ 20 mL and pH 3.0) with predicted methyl orange (MO) percent removal 68.1%. Considering the efficiency of the degradation process was significantly high even by using small quantities of this photocatalyst. With regard to the above-mentioned facts this method can be assumed as an applicable way to remove Methyl orange from wastewaters.

References

1. Zhao Y, Ma Y, Li H, Wang L (2012) Composite QDs@MIP Nanospheres for Specific Recognition and Direct Fluorescent Quantification of Pesticides in Aqueous Media. Anal Chem 84(1): 386-395.

2. Matsui J, Akamatsu K, Nishiguchi S, Miyoshi D, Nawafune H, et al. (2004) Composite of Au Nanoparticles and Molecularly Imprinted Polymer as a Sensing Material. Anal Chem 76(5): 1310-1315.

3. Tokonami S, Shiigi H, Nagaoka T (2009) Review: Micro- and nanosized molecularly imprinted polymers for high-throughput analytical applications. Anal Chim Acta 641(1-2): 7-13.

4. Xu L, Pan J, Xia Q, Shi F, Dai J, et al. (2012) Composites of Silica and Molecularly Imprinted Polymers for Degradation of Sulfadiazine. J Phys Chem C116(48): 25309-25318.

5. Zhang W, Li Y, Wang Q, Wang C, Wang P, et al. (2013) Performance evaluation and application of surface-molecular-imprinted polymer-modified TiO_2 nanotubes for the removal of estrogenic chemicals from secondary effluents. Environ Sci Pollut Res 20 (3): 1431-1440.

6. Gonzato C, Courty M, Pasetto P, Haupt K (2011) Magnetic Molecularly Imprinted Polymer Nanocomposites via Surface-Initiated RAFT Polymerization. Adv Funct Mater 21(20): 3947-3953.

7. Liu Y, Huang Y, Liu J, Wang W, Liu G, et al. (2012) Superparamagnetic surface molecularly imprinted nanoparticles for water-soluble pefloxacin mesylate prepared via surface initiated atom transfer radical polymerization and its application in egg sample analysis. J Chromatogr A 1246: 15-21.

8. Lu CH, Wang Y, Li Y, Yang H-H, Chen X, et al. (2009) Bifunctional superparamagnetic surface molecularly imprinted polymer core-shell nanoparticles. J Mater Chem 19(8):1077-1079.

9. Yu CL, Zhou WQ, Yu JC, Liu H, Wei LF (2014) Design and fabrication of heterojunction photocatalysts for energy conversion and pollutant degradation. Chin J Catal 35(10): 1609-1618.

10. Wang HL, Zhang LS, Chen ZG, Hu JQ, Li SJ, et al. (2014) Semiconductor heterojunction photocatalysts: design, construction, and photocatalytic performances. Chem Soc Rev 43(5): 5234-5244.

11. Moniz SA, Shevlin SA, Martin DJ, Guo ZX, Tang JW (2015) Visible-light driven heterojunction photocatalysts for water splitting – a critical review. Energy Environ Sci 8(6): 731-759.

12. Cao S, Chen G, Hu X, Yue PL (2003) Catalytic wet air oxidation of wastewater containing ammonia and phenol over activated carbon supported Pt catalysts. Catal Today 88 (1-2): 37-47.

13. Jiang H, Fang Y, Fu Y, Guo QX (2003) Studies on the extraction of phenol in wastewater. J Hazard Mater B 101(2): 179-190.

14. United States Environmental Protection Agency (USEPA) (1985) Technical support document for water quality based toxics control: EPA/440/485032. USEPA, Washington, DC.

15. Taguchi G (1986) Introduction to Quality Engineering: Designing Quality into Products and Processes. Asian Productivity Organization, Tokyo.

16. Saad H, Waleed IM, El A, Hager Ali R, Mona M (2015) Green synthesis and characterization of ZnO nanoparticles for photocatalytic degradation of Anthracene. Adv NatSci Nanosci Nanotechnol 6(4): 5012-5020.

17. Zolgharnein J, Asanjrani N, Bagtash M, Azimi G (2014) Multi-response optimization using Taguchi design and principle component analysis for removing binary mixture of alizarin red and alizarin yellow from aqueous solution by nano Y-alumina. Spectrochim Acta A Mol Biomol Spectrosc 126: 291-300.

18. Beril Gonder Z, Kaya Y, Vergili I, Barlas H (2010) Optimization of filtration conditions for CIP wastewater treatment by nanofiltration process using Taguchi approach. Sep Purif Technol 70(3): 265-273.

19. Mohaghegh N, Rahimi E, Gholami MR (2015) Ag3PO4/BiPO4 p–n heterojunction nanocomposite prepared in room-temperature ionic liquid medium with improved photocatalytic activity Mater Sci Semicond Process 39: 506-514.

20. Song YX, Zhu JX, Xu H, Wang C, Xu YG, et al. (2014) Synthesis, characterization and visible-light photocatalytic performance of Ag2CO3 modified by graphene-oxide. J Alloys Compd 592: 258-265.

21. Nabais JMV, Suhas JAG, Carrott Laginhas PJM, Roman CS (2009) Phenol removal onto novel activated carbons made from lignocellulosic precursors: influence of surface properties. J Hazard Mater 167(1-3): 904-910.

22. Hong SS, Ju CS, Lim CG, Ahn BH, Lim KT, et al. (2001) A photocatalytic degradation of phenol over TiO2 prepared by sol-gel method. J Indust Eng Chem 7(2): 99-104.

23. Hashim HAA, Mohamed AR, Lee KT (2012) Solar photocatalytic degradation of tartrazine using titanium dioxide. Jurnal Teknologi 35: 31-40.

24. Akyol A, Yatmaz HC, Bayramoglu M (2004) Photocatalytic decolorization of remazol red RR in aqueous ZnO suspensions. Applied Catalysis B: Environ 54(1): 19-24.

25. Byrappa K, Subramani AK, Ananda S, Rai KL, Dinesh R, et al. (2006) Photocatalytic degradation of rhodamine B dye using hydrothermally synthesized ZnO. Bulletin Mat Sci 29(5): 433-438.

26. Akpan UG, Hameed BH (2009) Parameters affecting the photocatalytic degradation of dyes using TiO2-based photocatalysts: A review. J Hazardous Mat 170(2-3): 520-529.

27. Inamdar J, Singh SK (2008) Photocatalytic detoxification method for zero effluent discharge in dairy industry: Effect of operational parameters. Int J Chem Biol Eng 2(1): 160-164.

28. Hager R Ali (2017) Photocoupling of Ag_3PO_4-Ag_2CO_3 with molecularly imprinted Polymer for enhanced removal of phenol under solar light: Application of Taguchi method. Int J Appl Eng Res 12(12): 3353-3359.

29. Katnanipa W (2017) Exploitation of Ag3PO4 Impregnated Alginate Beads for the Photocatalytic Degradation of Dye Solution under Sunlight Irradiation. Key Eng Mat 751: 689-694.

30. Maureira A, Rivas BL (2009) Metal ions recovery with alginic acid coupled to ul-trafiltration membrane. Eur Polym 45(2): 573-581.

31. Al-Sayed A, Yasser M, Eman A, Mohamed M, Mostafa MH (2015) Removal of ferrous ions from their aqueous solutions onto NiFe2O4–alginate composite beads. J Environ Chem Eng 3(3): 1486-1496.

32. Al-Sayed A, Yasser M, Eman A, Mohamed M, Mostafa MH (2015) Magnetic nanocomposite beads: synthesis and uptake of Cu(II) ions from aqueous solutions. Canad J Chem 93(3): 289-296.

33. Kiran B, Thanasekaran K (2011) Copper biosorption on Lyngbya putealis: application of response surface methodology (RSM). Int Biodeterior Biodegrad 65(6): 840-845.

34. Wenjun F, Ping W, Bing Y, Fengling Y, Dapeng L, et al. (2015) Ag3PO4/Ag2CO3 p–n heterojunction composites with enhanced photocatalytic activity under visible light. Chinese J Cataly 36(12) 2186-2193.

35. Sarkar S, Chakraborty S, Bhattacharjee C (2015) Photocatalytic degradation of pharmaceutical waste by alginate supported TiO2 nanoparticles in packed bed photo reactor (PBPR). Ecotox Environ Safe 121: 263-270.

36. Ngah WS, Ab Ghani S, Kamari A (2005) Adsorption behaviour of Fe(II) and Fe(III) ions in aqueous solution on chitosan and cross-linked chitosan beads. Bioresour Technol 96(4): 443-450.

37. Hassan AF, Abdel-Mohsen AM, Fouda MM (2014) Comparative study of calcium alginate, activated carbon, and their composite beads on methylene blue adsorption. Carbohydr Polym 102: 192-198.

38. Bakr AA, Mostafa MS, Eshaq G, Kamel MM (2014) Kinetics of uptake of Fe(II) from aqueous solutions by Co/Mo layered double hydroxide (Part 2). Desalin Water Treat 56(1): 248-255.

39. Limousin G, Gaudet J, Charlet L, Szenknect S, Barthes V, et al. (2007) Sorption isotherms: a review on physical bases, modeling and measurement. Appl Geochem 22(2): 249-275.

40. Siwei X, Man L, Junbao Y, Zhenghui Z, Hua W, et al. (2018) Immobilization of Ag3PO4 nanoparticles on chitosan fiber for photocatalytic degradation of methyl orange. Cellulose 25 (9): 5007-5015.

41. Yang LY, Dong SY, Sun JH, Feng JL, Wu QH, et al. (2010) Microwave-assisted preparation, characterization and photocatalytic properties of a dumbbell-shaped ZnO photocatalyst. J Hazard Matter 179(1-3): 438-443.

42. Song L, Li Y, Tian H, Wu X, Fang S, et al. (2014) Synthesis of AgBr/Ag4P2O7 compositephotocatalyst and enhanced photocatalytic performance. Mater Sci Eng B 189: 70-75.

43. Ge M, Zhu M, Zhao N, Li YP, Liu L (2012) Sunlight-assisted degradation of dye pollutants inAg3PO4 suspension. Ind Eng Chem Res 51(14): 5167-5173.